

Paradoxical Results of Long-Term Potentiation explained by Voltage-based Plasticity Rule

Abbreviated title: Voltage-based Plasticity Rule

Claire Meissner-Bernard (1), Matthias Tsai (2), Laureline Logiaco (3), Wulfram Gerstner (2)

(1) Friedrich Miescher Institute for biomedical research, 4058 Basel, Switzerland

(2) EPFL, 1015 Lausanne, Switzerland

(3) Columbia University, Center for Theoretical Neuroscience, 10027 New York, USA

Corresponding author: claire.meissner-bernard@fmi.ch

Number of pages: 18

Number of figures, tables, multimedia, and 3D models (separately): 7 figures and 3 tables

Number of words for abstract, introduction, and discussion (separately):

- Abstract: 170
- Introduction: 643
- Discussion: 1482

Conflict of interest statement: The authors declare no competing interest.

Acknowledgments: We thank Federico Brandalise and Friedemann Zenke for careful reading and critical comments on the manuscript. We thank Federico Brandalise and Johannes Letzkus for providing additional voltage traces. This research was supported by Swiss National Science Foundation (no.200020_184615) and by the European Union Horizon 2020 Framework Program under grant agreement no. 785907 (HumanBrain Project, SGA2).

Abstract

Experiments have shown that the same stimulation pattern that causes Long-Term Potentiation in proximal synapses, will induce Long-Term Depression in distal ones. In order to understand these, and other, surprising observations we use a phenomenological model of Hebbian plasticity at the location of the synapse. Our computational model describes the Hebbian condition of joint activity of pre- and postsynaptic neuron in a compact form as the interaction of the glutamate trace left by a presynaptic spike with the time course of the postsynaptic voltage. We test the model using experimentally recorded dendritic voltage traces in hippocampus and neocortex. We find that the time course of the voltage in the neighborhood of a stimulated synapse is a reliable predictor of whether a stimulated synapse undergoes potentiation, depression, or no change. Our model can explain the existence of different -at first glance seemingly paradoxical- outcomes of synaptic potentiation and depression experiments depending on the dendritic location of the synapse and the frequency or timing of the stimulation.

Significance statement

Memory is thought to be formed through plasticity of synapses. There have been numerous experiments investigating synaptic plasticity, sometimes leading to results which seem contradictory and suggest different learning rules for different experiments. However, theoretical models should eventually formulate unifying principles so that a single rule can explain a wide variety of results. Here we show that a voltage-based plasticity rule predicts experimentally measured plasticity, both in neocortex and allocortex, from experimental voltage traces recorded close to the 'plastic' synapse. Therefore, our work indicates that the time course of the postsynaptic voltage - which depends on the morphology and ion channels of the neuron - is an excellent indicator of whether or not changes are induced in stimulated synapses.

1. Introduction

How are memories encoded in the brain? Following earlier work of Richard Semon (1921), Donald Hebb postulated that a synapse connecting two neurons strengthens if both neurons are active together (Hebb, 1949), suggesting a concrete rule for the formation of memory traces. Experimentally, long-term potentiation (LTP) or long-term depression (LTD) are induced through an interaction of two signals, triggered by presynaptic and postsynaptic activities, respectively (Levy and Stewart, 1983; Bliss and Collingridge 1993; Sjostrom et al. 2001; Wang et al. 2005). Classical views on plasticity have linked the presynaptic signal to binding of neurotransmitters at postsynaptic receptors whereas the critical postsynaptic signal might be related to voltage (Artola et al., 1990), calcium (Cormier et al., 2001; Shouval et al. 2002), or backpropagating action potentials (Markram et al. 1997b).

A finding that challenges classical models of spike-timing dependent plasticity (STDP; Gerstner et al. 1996, Song et al. 2000, Kistler and van Hemmen, 2000) or frequency-based plasticity (Bienenstock et al., 1982) is the observation that plasticity rules depend on synapse location (Froemke et al., 2005, Letzkus et al., 2006). Another challenge for some (Gerstner et al., 1996; Song et al., 2000; Kistler and van Hemmen, 2000), but not all (Senn et al., 2001, Pfister and Gerstner, 2006; Clopath et al. 2010; Graupner and Brunel, 2012) STDP models is the interaction of frequency dependence and spike-timing dependence so that LTP for pre-before-post timing disappears at low frequencies (Sjostrom et al., 2001; Senn et al., 2001). A third challenge for all STDP and frequency-based Hebbian models is the observation of

subthreshold plasticity in the absence of somatic spikes (Ngezahayo et al., 2000; Golding et al., 2002; Brandalise et al., 2014; Lisman, 2005). We refer to these challenges as paradoxical effects of synaptic plasticity and ask whether a single phenomenological model can account for all of these.

Dendritic spikes have been shown to play a key role for the induction of plasticity in various brain regions (Holthoff et al., 2004; Kampa et al., 2006 and 2007; Gambino et al., 2014; Remy & Spruston, 2007). Dendritic events are linked to active channel properties which can vary along the dendritic tree (Spruston, 2008). Local dendritic nonlinearities could thus explain why different learning rules can be obtained with similar protocols in different brain regions or even within the same cell as a function of synapse location. However, most of the biophysical and phenomenological plasticity rules proposed over the years have been tested using simplified neuron models. Furthermore, for the class of plasticity models where the relevant postsynaptic variable is the dendritic voltage, a much more stringent test of plasticity models is possible, if the time course of the voltage in the neighborhood of the synapse is available.

In this paper we investigate whether a phenomenological model of synaptic plasticity in which the arrival of neurotransmitter is paired with the postsynaptic voltage at the location of the synapse can explain the aforementioned paradoxical experimental results (inversion of a plasticity rule as a function of dendritic location, LTP in the absence of somatic spikes and the interaction of spike-timing and spike frequency). We focus on three experiments where the time course of dendritic voltage was measured during the application of a plasticity-inducing protocol (in neocortex, Letzkus et al., 2006 and in hippocampus, Brandalise et al., 2014 and Brandalise et al., 2016). We hypothesize that the time-course of the postsynaptic voltage in the neighborhood of the synapse, in combination with presynaptic signaling is a reliable predictor of Hebbian synaptic plasticity and sufficient to explain the outcome of the experiments. Our model can be seen as a variation of earlier phenomenological voltage-based (Brader et al. 2007; Clopath et al., 2010) and calcium-based plasticity models (Shouval et al., 2002; Rubin et al., 2005; Graupner and Brunel, 2012). We show that our voltage-based model replicates plasticity behaviors of synapses across various dendritic locations in neocortex and hippocampus.

2. Results

Voltage dependence of plasticity

Our model combines ideas from phenomenological models of voltage-based plasticity (Brader et al. 2007, Clopath et al, 2010) with the 'veto' concept of Rubin et al. (2005). As described in the Methods section, each presynaptic spike leaves, in our model, a trace \bar{x} at the synapse; analogously, the activity of the postsynaptic neuron also leaves two traces at the synapse, described as two filtered version \bar{u}_+ and \bar{u}_- of the dendritic voltage u . Potentiation occurs if the variable \bar{u}_+ (i.e., the voltage low-pass filtered with time constant τ_+) is above some threshold θ_+ for potentiation, while the trace \bar{x} left by a presynaptic spike is non-zero. Similarly, depression occurs if \bar{u}_- (i.e., the voltage filtered with time constant τ_-) is above some threshold θ_- for depression, while \bar{x} is non-zero (Figure 1A-C). Importantly, to translate the competition between the molecular actors (phosphatase vs. kinase) involved in LTP and LTD (Bhalla and Iyengar 1999; Lee et al. 2000, Xia et al. 2005, Herring et al. 2016) into mathematical equations, we introduce into our model a 'veto' concept: when potentiation occurs, the value of θ_- is increased. Thus, a potentiation signal overwrites LTD that would occur otherwise (Rubin et al. 2005; O'Connor et al., 2005; Cho et al., 2001). In our model the veto mechanism is implemented by a dynamic increase of the LTD-threshold θ_- that is characterized by parameters b_θ and τ_θ .

If we pair presynaptic stimulation with a constant voltage at the location of the synapse, our model shows three regimes (Figure 1D-G): (i) for hyperpolarization or voltage close to rest, synapses do not show any plasticity; (ii) for voltages above a first threshold θ_0 , presynaptic stimulation leads to a depression of the synapses; (iii) for voltages above a second threshold θ_1 the synapses exhibit potentiation. Our model is consistent with experimental results of Ngezhahayo et al. (2000) who paired 2 Hz presynaptic stimulations with constant postsynaptic depolarizations (voltage clamp) and determined the stationary voltage–plasticity function for the induction of LTD and LTP. For a wide range of parameter choices, our model qualitatively reproduces this stationary voltage dependence, if we assume that during clamping the voltage u at the dendrite is equal to the somatic voltage (Figure 1E-G).

In more realistic experiments, the voltage at the location of the synapse is not constant but changes as a function of time. In the following, we investigate if our model can reproduce the experimentally measured plasticity observed with various LTP or LTD-inducing protocols. For this purpose, we feed the voltage time course of experimental dendritic recordings into our plasticity model. Parameters of our model are fitted so that the plasticity predicted by our model matches as closely as possible the plasticity data observed in various experimental conditions. We focus on experimental paradigms (Letzkus et al., 2006; Brandalise et al., 2014, 2016) where the dendritic voltage was recorded close to the stimulated synapse during plasticity induction. We now study these paradigms in more detail.

Subthreshold plasticity in the hippocampus

Brandalise et al. (2014) investigated plasticity at CA3 recurrent synapses in rat hippocampus using a subthreshold pairing protocol (Figure 2A): an EPSP of a few millivolts induced by stimulation of the CA3 recurrent pathway was paired (60 pairings at 0.1Hz) with a subthreshold mossy fibre (MF) stimulation that, if stimulated separately, also led to an EPSP of a few millivolts. No action potentials (AP) were generated in the CA3 cell. We copied the dendritic voltage time course from 3 cells into our plasticity model (data kindly shared by F. Brandalise). The voltage time course combined with plasticity outcome were available for 5 different protocols, which were performed in the following order:

1. There was no MF stimulation (CA3 alone). The dendritic voltage reflected the small EPSP caused by stimulation of the recurrent synapse. No plasticity was observed (Figure 2C). Protocol 1 was available for cells 2 and 3.
2. the MF and CA3 stimulations occurred at the same time (0 ms). The dendritic voltage contained contributions of inputs from MF and CA3, but no plasticity was observed (Figure 2C). Protocol 2 was available for all three cells
3. the MF stimulation followed the CA3 stimulation with a 10 ms time interval (+10 ms) in the absence of any pharmacological manipulation (Figure 2B and C). This is the most interesting paradigm that is discussed in the next paragraph. Protocol 3 was available for all three cells.
4. the MF stimulation followed the CA3 stimulation with a 10 ms time interval (+10 ms), but in the presence of AP5, an NMDA receptor antagonist, or while holding the cell at -90 mV. No plasticity was observed (Figure 2C). Protocol 4 was available for cells 1 and 3.
5. the MF stimulation preceded the CA3 stimulation with a 40 ms interval (-40 ms). The dendritic voltage contained contributions of inputs from MF and CA3 and LTD was observed (Figure 2B and C). Protocol 4 was available for cells 1 and 3.

Repetitive pairings during the +10 ms protocol (protocol 3) induced two types of dendritic voltage trajectories: either a nearly linear addition of the EPSPs caused by MF and CA3 stimulation or a strongly supralinear voltage response (see Figure 2B and Brandalise et al., 2014). In all cells, the mean amplitude of the supralinear events, calculated in relation to linear event amplitude was increased by at least a factor of two (i.e., difference 100% or more, Table

1, column 3). This indicates that (i) nonlinear effects are strong and (ii) the dendritic recording electrode was close enough to the stimulated CA3 recurrent synapses to pick up such a nonlinear effect (see Brandalise et al., 2014). Importantly, a given cell could exhibit in one repetition of the stimulation a linear response, and the same cell could then show in the next repetition a supralinear response. The percentage of supralinear events that occurred during this protocol for each cell is given in Table 1. The occurrence of supralinear events was completely blocked by AP5 infusion or holding the cell at -90 mV (protocol 4, Table 1).

cell number	rise time (ms)	% increase of amplitude beyond linear	% supralinear events		potentiation (EPSP amplitude change in %)	
			no block	block	no block	block
cell 1	4.2	130	34	0	122.0	95.5
cell 2	3.38	100	33.3	/	131.0	/
cell 3	6.72	140	27	0	119.3	104.3

Table 1. Protocol 3 and 4 (+10ms) for cells 1-3. Rise time of EPSP, increase of EPSP amplitude during supralinear events, percentage of supralinear events and amount of potentiation of the 3 recorded cells. The occurrence of supralinear events was completely blocked by AP5 infusion (“block”, cell 1) or holding the cell at -90 mV (“block”, cell 3). The % increase in amplitude is defined as the difference between the amplitude a_s of the supralinear events and the amplitude a_l of the linear events, divided by the amplitude of the linear events: $\% = 100(a_s - a_l) / a_l$. Note that a value of 100 indicates a maximum voltage twice as high as predicted by linear summation.

We found that our model with a fixed set of parameters could reproduce the outcome of this sequence of experiments for all three cells (see Figure 2C). Importantly, in order to predict the plasticity outcome for a given cell, we used the dendritic voltage recorded for that specific cell. Hence variations in the amount of plasticity during protocol 3 are explained in the model by changes in the voltage recordings – without any changes of parameters between different cells. The set of parameters in Table 2 was obtained with all available voltage traces corresponding to 12 plasticity outcomes, using an optimization algorithm which minimized the mean-squared error (difference between theoretical and experimental plasticity squared, see Methods).

In order to control against overfitting we used an additional, independent, optimization procedure (leave-one-out cross-validation): we fitted the model parameters on plasticity outcomes for 11 voltage traces by minimizing the mean-squared error and predicted the plasticity outcome on the remaining one (see Table 3 for the statistics over all 12 leave-one-out experiments). Even though the median error after testing the plasticity outcome on the excluded voltage traces was (as expected) larger than the median training error (Table 3), its actual value of 6.4×10^{-4} (Table 3) was comparable to the error of 7.6×10^{-4} observed in the direct fitting approach (Table 2). Furthermore, we found that most parameter values are consistent across the 12 leave-one-out experiments as indicated by a small standard deviation of the parameter value compared to its mean value (Table 3); exceptions were the parameters of the plasticity amplitudes A_{LTP} and A_{LTD} and the veto parameters b_0 and τ_0 which showed rather large standard deviations. A sensitivity analysis (Figure 3) indicated that the exact values of these four parameters was not critical (Figure 2D). Thus, cross-validation and sensitivity analysis confirm that the model has predictive power.

To understand how the model works, let us focus on a few examples (Figure 2B). During the -40 ms protocol (protocol 5), the low-pass filtered voltage trace \bar{u}_+ did not reach the threshold θ_+ for LTP induction, whereas the voltage \bar{u}_- filtered with a larger time constant reached θ_- , inducing LTD (Figure 2B). With the +10 ms protocol (protocol 3), \bar{u}_+ reached θ_+ only during trials in which a supralinear event occur (Figure 2B). During linear events and similarly when AP5 was infused, \bar{u}_+ and \bar{u}_- did not reach their respective thresholds θ_+ and θ_- . It should be noted that LTP induction during the supralinear events blocked LTD induction through the veto signal manifesting itself as an increase of the LTD threshold θ_- (Figure 2B, middle panel).

To further test the ability of our model to predict plasticity at CA3 recurrent synapses, we used the results of Brandalise et al. (2016) obtained with a classic STDP protocol. They paired a recurrent CA3 EPSP with 3 APs at 200 Hz (10 ms time interval, 50 pairings at 0.3Hz, see Figure 4). This stimulation led in more than half of the trials to the generation of a dendritic spike (Figure 4B), unless a hyperpolarizing step current was applied in the dendrite during the brief somatic injections triggering the APs (Figure 4C). Similarly, pairing the CA3 EPSP with 3 APs at 50 Hz or with a single AP did not generate a dendritic spike (Figure 4D).

We wondered whether our model would be able to reproduce these experimental results. Even though experiments of Brandalise et al. (2016) were done at the same synapse type as those of Brandalise et al. (2014), we allowed for small variations of the parameters' values relative to the best model of the data of Brandalise et al. (2014) in order to account for small changes in preparation (composition of the external solution). In order to decide which parameters were allowed to change compared to Brandalise et al. (2014) data, we made use of the sensitivity analysis (Figure 2D). The more sensitive parameters τ_+ , τ_x , θ_+ , θ_0 were allowed to vary in a range of plus or minus 35% whereas the remaining five parameters (i.e., time constant τ_- , plasticity amplitudes A_{LTP} and A_{LTD} , as well as veto parameters b_θ and τ_θ) were kept fixed at the value found in the previous experiment. We found that with adjusted parameters, our model could account for the outcome of the STDP experiments in Brandalise et al. 2016 (see Figure 4 and Table 2).

	τ_x ms	τ_+ ms	θ_+ mV	θ_0 mV	A_{LTP} 10^{-5} $mV^1.ms^{-1}$	A_{LTD} 10^{-5} $mV^1.ms^{-1}$	τ_- ms	b_θ 10^4 mV.ms	τ_θ ms	error
Letzkus	22.4	2.00	27.1	6.20	4.28	16.4	60.0	1.00	29.1	$7.2 \cdot 10^{-2}$
Branda, subthreshold	7.09	6.38	8.12	5.18	356	382	15.5	3.00	6.76	$7.6 \cdot 10^{-4}$
Branda, STDP	4.90	8.58	10.9	6.55	356	382	15.5	3.00	6.76	$4.1 \cdot 10^{-4}$
Sjostrom	16.7	9.06	14.8	6.84	875	98	29.0	4.50	7.43	$2.3 \cdot 10^{-2}$

Table 2. Parameters giving the smallest error (see Methods). The error is defined as the squared difference between experimental and theoretical value.

LSE		Coefficient of variation (%)								
Training (normalized)	Testing	τ_x	τ_+	θ_+	θ_0	A_{LTP}	A_{LTD}	τ_-	b_θ	τ_θ
$0.17 \cdot 10^{-4}$	$6.4 \cdot 10^{-4}$	6.3	8.5	3.2	1.9	13	10	3.6	28	82

Table 3. Median error after training on 11 plasticity traces and testing on the 12th excluded one. Training is the averaged error divided by 11. We obtain 12 sets of best parameters after the cross-validation: we indicate here the coefficient of variation for each parameter ($sd/mean*100$).

Location-dependent plasticity in neocortical apical dendrites

Letzkus et al. (2006) investigated plasticity at both proximal and distal synapses between layer 2/3 and layer 5 pyramidal neurons in slices from rat somatosensory cortex. Observed plasticity rules varied in a paradoxical fashion depending on synapse location on the dendritic tree: Proximal EPSPs were potentiated during pairing with somatic bursts of APs occurring 10 ms after the onset of the EPSP (+10 ms) and depressed when the postsynaptic bursts occurred 10 ms before the EPSP (-10ms) ; at distal synapses, however, the pattern was reversed and EPSPs depressed during +10 ms pairings and were potentiated for -10 ms pairings (Letzkus et al., 2006).

Plasticity was measured as a function of the rise time of the somatic EPSP which correlated linearly with the distance of the synapse to the soma (Letzkus et al., 2006). We extracted the averaged plasticity value corresponding to synapses located 100, 330 and 660 μm from the soma and asked whether our voltage-based plasticity model was able to predict the plasticity results. To answer this question, we fed our plasticity model with representative dendritic voltage traces (Figure 5A) recorded close to synapses located 100 μm (proximal), 330 μm or 660 μm (distal) away from the soma (Letzkus et al., 2006 and personal data from J. Letzkus). We found that our voltage-based plasticity model with a single set of parameters could account for the plasticity results at both proximal and distal synapses (see Figure 5B and Table 2). Moreover, the model with the same set of parameters could also explain why distal EPSPs did no longer potentiate after pairing at -10ms but still depressed (Figure 5D) during pairing at +10 ms, if the amplitude of the dendritic spikes evoked by the AP bursts decreased due to the presence of NiCl_2 (a blocker of a subtype of voltage-gated calcium channels, Figure 5C and Letzkus et al. 2006).

To understand our results, let us focus on Figure 6. At distal synapses, during +10 ms pairings, the value of the presynaptic trace \bar{x} had already decreased significantly when \bar{u}_+ reached the threshold θ_+ (Figure 6A). The amount of LTP was not high enough for the veto to have a significant impact on LTD induction. In contrast, for -10 ms pairings, \bar{x} switched from 0 to its maximal value 1 at a moment when \bar{u}_+ was close to its maximal value well above θ_+ (Figure 6B). Therefore, the amount of LTP induced was high. The large LTP signal vetoed the induction of LTD as manifested by an increase in the LTD threshold θ_- . However, in the presence of NiCl_2 , the difference between \bar{u}_+ and θ_+ was significantly reduced compared to the control case, leading to a behavior of the plasticity model similar to that described for the +10ms pairings.

Thus, the results of our voltage-based plasticity model support the idea that differences in the voltage traces can explain the spatial differences in the learning rule, as suggested by Letzkus et al. (2006). Importantly, all the above experiments are explained by the same model with the same set of parameters.

High-frequency pairings in neocortical basal dendrites

We have until now focused on plasticity results obtained after repeated pairings of pre and postsynaptic activities at a low frequency (0.1 and 1 Hz). Yet, an important feature of synaptic plasticity is its frequency-dependence. Different amounts of plasticity are obtained by repeating the same pairings at different frequency. Unfortunately, experimental dendritic recordings are not available for these types of experiments. Results have been obtained among others at L5-L5 synapses of rat neocortical neurons (Sjostrom et al., 2001), which are well-characterized. More than half of the synaptic contacts between L5 neurons are made on basal dendrites ($80 \pm 35 \mu\text{m}$ from the soma in young rats, Markram et al., 1997a). We simulated dendritic voltage around $80 \mu\text{m}$ from the soma using the model of L5 basal dendrites of Nevian et al. (2007) at four different frequencies (0.1, 10, 20 Hz and 40 Hz) and with different time intervals between the presynaptic and the postsynaptic stimulation (-10, 0 +10 and +25 ms). As shown in Figure 7, our model with fixed set of parameters can reproduce both the frequency-dependence and spike-timing dependence of plasticity.

To summarize, the same voltage-based plasticity model can account for four different series of experiments corresponding to four publications (Brandalise et al. 2014, 2016; Letzkus et al., 2006; Sjostrom et al., 2001). Importantly, the model parameters are slightly different for different synapse types or preparations (i.e., different publications), but each series of experiments is explained by a single set of model parameters (Table 2). These model parameters are kept fixed across all experimental results in a given publication.

3. Discussion

Long-term potentiation or long-term depression are induced through the combined action of the presynaptic and postsynaptic activities. We showed that a single phenomenological voltage-based model could explain results using various synaptic plasticity protocols: experiments (i) with voltage clamp (Figure 1); (ii) with variable time interval between presynaptic and postsynaptic spikes (Figures. 2,5,7); (iii) with variable pairing frequency (Figure 7); (iv) with multiple postsynaptic spikes (Figures 4,5,7); (v) with subthreshold plasticity (Figure 2) and (vi) with location-dependence (Figure 5).

Comparison with other plasticity models

Voltage-based models (Brader et al., 2007; Clopath et al., 2010) are built on correlations of presynaptic spike arrival with postsynaptic voltage. Calcium-based models (Shouval et al. 2002; Rubin et al. 2005; Graupner et al., 2012) are built on changes in calcium concentration over time, with different thresholds leading to LTP or LTD. All of these models, as well as the model proposed here, are phenomenological ones since they do not aim to describe the full mechanistic signaling chain from presynaptic spike arrival to a change in the number of AMPA receptors or presynaptic release probabilities but rather provide a 'shortcut' in the form of a compressed 'learning rule' with only a few variables.

How does the presynaptic variable (such as arrival of the neurotransmitter glutamate at postsynaptic receptors) interact with the postsynaptic variable, such as calcium or voltage? In calcium-based models (Shouval et al. 2002, Rubin et al. 2005, Graupner et al 2012), presynaptic activity induces synaptic currents into the postsynaptic neuron and an influx of

calcium through NMDA channels. Further changes of the calcium concentration occur because of postsynaptic activity such as a backpropagating action potential via voltage-gated ion channels or buffers. The level (Shouval et al., 2002) or time course (Rubin et al., 2005, Graupner et al. 2012) of the calcium concentration in the simulated model is then compared with threshold variables in order to predict occurrence of LTP or LTD. Rubin et al., (2005) proposed to add a "veto" of LTP on LTD when a relatively high calcium threshold was reached which inspired the veto mechanism in the present model. Importantly, calcium concentration acts as a summary variable that includes effects of both pre- and postsynaptic activity.

In voltage-based models (Brader et al., 2007; Clopath et al., 2010), presynaptic activity leaves a filtered trace at the synapse which we interpret as the amount of glutamate bound to the postsynaptic receptor. In these voltage-based model, and similarly in our model, it is this glutamate trace that interacts with postsynaptic voltage, either with the voltage directly or with a low-pass filtered version thereof. The comparison of the voltage variables with several thresholds allows to predict the induction of LTP or LTD of those synapses that have been presynaptically stimulated (Brader et al., 2007; Clopath et al., 2010). Thus voltage-based models jump over the biophysics of calcium dynamics and connect the presynaptic stimulation in combination with the time course of the postsynaptic voltage directly with the outcome of plasticity experiments.

For LTD induction, Clopath et al., (2010) combine an instantaneous spike event, rather than the glutamate trace, with a low-pass filtered version of the postsynaptic voltage. However, in our model, LTD is triggered by the joint action of the glutamate trace and postsynaptic voltage. Using a glutamate trace (as opposed to a presynaptic spike event that covers a much shorter moment in time) is in our hands the only way to make LTD possible for pre-before-post pairings at low pairing frequencies (see Letzkus et al., 2006 as an example). Also, an extended glutamate trace looks biologically more plausible than a "point-like event" assumed in some classic STDP models (Kister and van Hemmen, 2000; Song et al., 2000).

Another main difference between Clopath et al., (2010) and our model is the absence of a quadratic voltage term. In Clopath et al., (2010), two conditions need to be met for LTP induction: the momentary voltage $u(t)$ needs to be above the threshold θ_+ and the low-pass filtered voltage \bar{u}_+ needs to be above θ_- . The high voltage during an action potential meets the condition " $u(t)$ above θ_+ ", but for LTP to be induced, the (low-pass filtered) membrane potential must already be depolarized before the spike (" \bar{u}_+ above θ_- ", for example by a depolarizing spike after-potential due to earlier spikes or by a subthreshold depolarizing input, see Sjostrom et al. 2001). The two conditions together imply a quadratic dependence on voltage in the LTP inducing term (Clopath et al., 2010). Instead of a quadratic voltage term of LTP induction, our model works with a linear dependence on the low-pass filtered voltage in combination with a veto-mechanism similar to the one suggested by Rubin et al. (2005).

Previous models were able to quantitatively fit the frequency dependence of STDP (Senn et al., 2001) as well as triplet and quadruplet effects of STDP protocols (Pfister and Gerstner, 2005; Clopath et al., 2010; Graupner and Brunel., 2012). The model of Graupner and Brunel (2012) also indicated how changes of STDP rules as a function of synaptic location on the dendrite could be qualitatively accounted for by changes of model parameters; in the absence of dendritic recordings and an appropriate dendrite model, a quantitative fit was not to be expected. Our voltage-based models is probably the first one to directly link dendritic voltage recordings with plasticity outcome, bypassing the need for a biophysically correct dendrite model.

Role of dendritic plateau potentials

Letzkus et al. (2006) showed that at distal locations, the peak amplitude of isolated backpropagating action potentials was half the size than that at proximal locations.

Furthermore, postsynaptic bursts at the soma generated dendritic calcium spikes at distal locations. The two observations suggest that the somatic spike is less important for plasticity in distal dendrites than localized depolarizations at the location of the synapse. Similarly, in the hippocampal experiments of Brandalise et al. (2014 and 2016), dendritic NMDA spikes were generated: they resulted from high frequency bursting during the STDP protocol, and from broad and long mossy-fiber evoked EPSPs during the subthreshold protocol.

Both Letzkus et al. (2006) and Brandalise et al. (2014 and 2016) showed that long-term potentiation was abolished when dendritic spikes were blocked (pharmacologically or by hyperpolarizing the cell). In our model, the voltage time course at the location of the synapse determines whether or not LTP (or LTD) is induced at stimulated synapses. If the low-pass filtered voltage \bar{u}_+ does not reach a threshold θ_+ , then potentiation is impossible. In our model a prolonged dendritic plateau potential is more efficient than a short and isolated dendritic spike. Furthermore, dendritic nonlinearities can explain the existence of different – at a first glance seemingly paradoxical - outcomes of plasticity experiments. Since we paste the experimentally measured voltage traces directly into our plasticity model, the biophysical source of the depolarization does not matter.

Concluding Remarks and Predictions

We do not claim that elevated voltage in combination with neurotransmitter is the direct cause of induction of LTP or LTD. Rather our philosophy is that the voltage time course, if experimentally available, is a very good indicator of whether or not synaptic changes are induced in those synapses that have been presynaptically stimulated. In other words, our model describes the Hebbian condition of joint activity of pre- and postsynaptic neuron in a compact form as the interaction of the glutamate trace left by a presynaptic spike with the time course of the postsynaptic voltage. This philosophy does not exclude that a pharmacological block of later steps in the signaling chain could interrupt the LTP-induction or that a direct experimental manipulation of postsynaptic calcium could induce synaptic plasticity in the absence of presynaptic spike arrival or postsynaptic depolarization. Rather our intuition is that, under physiological conditions, the time course of the voltage in the neighborhood of a synapse is a reliable indicator of the likelihood of a stimulated synapse to undergo plasticity. Our leave-one-out cross-validation results (Table 3) show that this intuition can be transformed into a working model to predict the outcome of future plasticity induction experiments given the voltage trace.

Since our model is a phenomenological one (as opposed to a biophysical model that describes the full signal induction chain, e.g., Lisman and Zhabotinsky, 2001) it cannot be used as a predictive tool in cases where specific biochemical molecules are manipulated without affecting the voltage time course. However, one interesting qualitative prediction follows from the interaction of the veto-concept in our voltage based model. We predict a voltage-dependence of LTP induction (Figure 1D-E) which depends on the stimulation frequency of glutamate pulses. Since presynaptic vesicles are likely to deplete rapidly, we propose an experiment where presynaptic spike arrivals are replaced by glutamate puffs of standardized size while the postsynaptic voltage is clamped at a constant voltage. The prediction from our simple voltage-based model is that the voltage dependence of LTP induction becomes steeper at higher stimulation frequencies – even if the number of pulses is kept constant.

4. Methods

Voltage-based model of synaptic plasticity

The plasticity model (Figure 1) is a combination of earlier voltage-based models (Brader et al. 2007, Clopath et al. 2010) and the veto concept of Rubin et al., 2005.

Plastic changes of a synapse are caused by potentiation (LTP) or depression (LTD) of the synaptic weight w and add up to a total weight change

$$\frac{d}{dt}w(t) = \frac{d}{dt}w_{LTP} - \frac{d}{dt}w_{LTD}.$$

Potentiation or depression of the weight is induced by a Hebbian combination of presynaptic and postsynaptic activity. Postsynaptic activity is represented by the (low-pass filtered) voltage at the location of the synapse. Presynaptic activity is represented by the spike train $X(t)$ (a sequence of Dirac delta-pulses) arriving at the synapse. The spike train is low-pass filtered and gives rise to a 'trace'

$$\tau_x \frac{d}{dt}\bar{x}(t) = -\bar{x}(t) + X(t)$$

where \bar{x} can be thought of as the amount of neurotransmitter bound to the postsynaptic receptors. The value of \bar{x} increases at the arrival of a spike and decays exponentially with a time constant τ_x during the interval between spike arrivals (see Figure 1B).

Depression (LTD) is induced if a low-pass filtered version \bar{u}_- of the postsynaptic voltage is above a threshold θ_- while the "trace of presynaptic activity" \bar{x} is non-zero,

$$\frac{d}{dt}w_{LTD}(t) = A_{LTD}\bar{x}(t)[\bar{u}_-(t) - \theta_-]_+$$

where \bar{u}_- is defined as

$$\tau_- \frac{d}{dt}\bar{u}_-(t) = -\bar{u}_-(t) + u(t)$$

with time constant τ_- . The amplitude parameter A_{LTD} characterizes the magnitude of LTD. $[y]_+$ equals y if $y > 0$, 0 otherwise.

Potentiation (LTP) is induced if another low-pass filtered version \bar{u}_+ of the voltage is above a threshold θ_+ while the "trace of presynaptic activity" \bar{x} is non-zero,

$$\frac{d}{dt}w_{LTP}(t) = A_{LTP}\bar{x}(t)[\bar{u}_+(t) - \theta_+]_+$$

where \bar{u}_+ is defined as

$$\tau_+ \frac{d}{dt}\bar{u}_+(t) = -\bar{u}_+(t) + u(t)$$

with time constant τ_+ . The amplitude parameter A_{LTP} characterizes the magnitude of LTP.

Finally, depression and potentiation compete. If potentiation occurs, the threshold θ increases. The value of θ is determined by the following equation:

$$\theta_-(t) = \theta_0 + \theta(t)$$

with a fixed part θ_0 and a variable part $\theta(t)$ that follows the equation

$$\tau_\theta \frac{d\theta}{dt} = -\theta + b_\theta \frac{d}{dt} w_{LTP}$$

with time constant τ_θ and interaction parameter b_θ . This interaction of LTD and LTP parallels the 'veto' concept of the Rubin et al. 2005.

We assume that the plasticity framework defined by the above set of equations is generic for glutamatergic NMDA synapses whereas the specific choice of parameters for amplitudes, thresholds and time constants depends on the specific neuron and synapse type as well as on temperature and ion concentrations in the bath of the experimental slice preparation.

Postsynaptic voltage trace

In the above plasticity model, the value of the postsynaptic voltage at the location of the synapse plays a crucial role. We have access to three experimental datasets where voltage has been measured at a dendritic location close to the synapse. The first data set is from neocortex (Letzkus et al. 2006, containing 20 and 23 data points for the +10ms and -10 ms pairings, respectively, corresponding to the synapses at various locations along the dendritic tree) and the other two are from allocortex (Brandalise et al. 2014, 2016). Thus, for these plasticity experiments, we do not need to use a neuron model to generate voltage traces; rather, we directly insert a representative experimental voltage trace $u(t)$ into the equations of our plasticity model.

We also model results from Sjöström et al. 2001. In this case, we only had access to representative voltage traces measured at the soma. Since we need for our plasticity model voltage traces in the neighborhood of a synapse, we used the model of L5 basal dendrites from Nevian et al. (2007), available on ModelDB (#124394) to mimic dendritic voltage traces. The multicompartmental model was simulated in NEURON. Action potentials were generated by a 5 ms step current of 3 nA in the somatic compartment and backpropagated through Hodgkin-Huxley-like sodium and potassium channels located on the soma and dendrite. Unitary EPSPs were generated by activation of AMPA synapses (0.25 ms decay time constant and peak conductance of 1.5 nS).

All voltage traces (experimental ones and simulation-based ones) have been shifted to a resting potential to 0. This shift allows us to counteract any discrepancies in absolute voltage arising from the electrophysiological recording system or from differences in resting membrane potential across different brain regions and neuron types.

Parameter optimization

Our model only defines a mathematical framework whereas specific parameter values may depend on neuron type, synapse type, brain region, as well as details of slice preparations.

Therefore, we use different sets of parameters, depending on the experiments we want to model. We take (experimental or simulated) voltage traces as input to our model. Differential equations were solved using forward Euler and with an integration time step of 0.1 ms. Synaptic weights w were initialized at $w_i = 0.5$ and at the end of the simulation we read out the final value w_f .

The 9 parameters of our model were fitted to the outcome of different experiments using the Matlab function `fmincon` (interior-point algorithm). We fixed $\theta_+ > \theta_0$ and defined some upper and lower bounds for the parameters (see Table 4. Time constants are in milliseconds with lower bound always at 2ms and upper bounds at are below 100ms). In order to mitigate the problem of local minima, we used 25 predefined combinations of parameters as initial points for the optimization algorithm (all inside the bounds). We minimized the least squared error (LSE)

$$LSE = \sum_{protocols} \left(\frac{w_f - w_i}{w_i} - plasticity_{exp} \right)^2$$

defined as the squared difference between the theoretical value predicted by the model and the experimental value. Since we are interested in the optimal set of parameters, we report in the paper always the parameters from the optimization run which yielded the smallest LSE. We checked that an automatic generation of initial points did not alter the results.

bound	τ_x	τ_+	θ_+	θ_0	A_{LTP}	A_{LTP}	τ_-	b_θ	τ_θ
lower	2	2	5	2.5	10^{-5}	10^{-5}	2	0	2
upper	30	60	30	15	10^{-2}	10^{-2}	60	$5 \cdot 10^4$	100

Table 4. **Lower and upper bound used during the `fmincon` search**

Code availability

Code is available on GitHub at <https://github.com/clairemb90/Voltage-based-model>

5. References

Artola, A., Bröcher, S. and Singer, W. (1990) Different voltage dependent thresholds for inducing long-term depression and long-term potentiation in slices of rat visual cortex. *Nature* 347, pp. 69–72.

Bienenstock, E. L., Cooper, L. N., and Munroe, P. W. (1982). Theory of the development of neuron selectivity: orientation specificity and binocular interaction in visual cortex. *J. Neurosci.*, 2:32-48.

Bliss, T. V. P. and Collingridge, G. L. (1993) A synaptic model of memory: long-term potentiation in the hippocampus. *Nature* 361, pp. 31–39.

Brader, J., Senn, W., and Fusi, S. (2007). Learning real-world stimuli in a neural network with spike-driven synaptic dynamics. *Neural Comput.* 19, 2881–2912.

- Brandalise, F., Carta, S., Helmchen, F., Lisman, J. & Gerber U. (2016) Dendritic NMDA spikes are necessary for timing-dependent associative LTP in CA3 pyramidal cells *Nat.Comm.* 7:13480
- Brandalise, F. & Gerber U. (2014) Mossy fiber-evoked subthreshold responses induce timing-dependent plasticity at hippocampal CA3 recurrent synapses (2014) *PNAS* 111(11) 4303-4308.
- Cho, K., Aggleton, J. P. , Brown, M. W. & Bashir, Z. I. (2001) An experimental test of the role of postsynaptic calcium levels in determining synaptic strength using perirhinal cortex of rat, *Journal of Physiology*, 532.2, pp.459–466
- Clopath, C. & Gerstner W. (2010), Voltage and spike timing interact in STDP a unified model, *Frontiers in Synaptic Neuroscience* 2(25), 1
- Clopath, C., Busing, L., Vasilaki, E., & Gerstner, W. (2010). Connectivity reflects coding: a model of voltage based spike-timing-dependent plasticity with homeostasis. *Nat. Neurosci.* 13, 344-352.
- Cormier, R. J., Greenwood, A. C. & Connor, J. A. (2001) Bidirectional Synaptic Plasticity Correlated With the Magnitude of Dendritic Calcium Transients Above a Threshold *J. Neurophysiol.* 85, 399–406.
- Froemke, R.C., Poo M.M. & Dan, Y (2005) Spike-timing-dependent synaptic plasticity depends on dendritic location. *Nature* 434
- Gambino, F., Pages, S., Kehayas, V., Baptista D., Tatti, R., Carleton, A., & Holtmaat, A. (2014) Sensory-evoked LTP driven by dendritic plateau potentials in vivo. *Nature* 515, pages116–119
- Gerstner, W., Kempter, R., van Hemmen, J. L., and Wagner, H. (1996a). A neuronal learning rule for sub-millisecond temporal coding. *Nature*, 386:76-78.
- Golding, N.L. et al. (2002) Dendritic spikes as a mechanism for cooperative long-term potentiation. *Nature* 418, 326–331
- Graupner, M., & Brunel, N. (2012) Calcium-based plasticity model explains sensitivity of synaptic changes to spike pattern, rate, and dendritic location. *Proceedings of the National Academy of Sciences*: 201109359.
- Hebb, D. O. (1949). *The Organisation of Behavior*. New York:Wiley
- Herring, Bruce E., and Roger A. Nicoll. "Long-term potentiation: from CaMKII to AMPA receptor trafficking." *Annual review of physiology* 78 (2016): 351-365.
- Holthoff, K., Kovalchuk, Y., Yuste, R., & Konnerth, A. (2004). Single-shock LTD by local dendritic spikes in pyramidal neurons of mouse visual cortex: Dendritic spikes and LTD. *The Journal of Physiology*, 560(1), 27–36.
- Kampa, B., Letzkus, J. & Stuart, G. (2006). Requirement of dendritic calcium spikes for induction of spike-timing-dependent synaptic plasticity. *J. Physiol.* 574.1, 283-290.
- Kampa B.M., Letzkus J.J. & Stuart G.J. (2007) Dendritic mechanisms controlling spike-timing dependent synaptic plasticity. *Trends in Neurosciences* 30(9), 456
- Kistler, WM and van Hemmen JL (2000) Modeling synaptic plasticity in conjunction with the timing of pre- and postsynaptic action potentials. *Neural Computation* 12: 385
- Levy, W. B. & Stewart, D. (1983) Temporal contiguity requirements for long-term associative potentiation/depression in hippocampus. *Neurosci*, 8, pp. 791–797

Letzkus, J., Kampa, B., & Stuart, G. (2006). Learning rules for spike timing-dependent plasticity depend on dendritic synapse location. *J. Neurosci.* 26, 10420-10429

Lisman, J. & Spruston, N. (2005) Postsynaptic depolarization requirements for LTP and LTD: a critique of spike timing dependent plasticity. *Nature Neuroscience* 8(7), 839

Lisman, J. & Zhabotinsky A.M. (2001) A Model of Synaptic Memory: A CaMKII/PP1 Switch that Potentiates Transmission by Organizing an AMPA Receptor Anchoring Assembly, *Neuron* 31:191-201

Markram, H., Lübke, J., Frotscher, M., Roth, A., & Sakmann, B. (1997a), Physiology and anatomy of synaptic connections between thick tufted pyramidal neurons in the developing rat neocortex, *J. Physiology*, 500:409-440

Markram, H., Lübke, J., Frotscher, M. & Sakmann, B. (1997b) Regulation of synaptic efficacy by coincidence of postsynaptic AP and EPSP. *Science* 275, pp. 213–215.

Nevian et al. (2007) Properties of basal dendrites of layer 5 pyramidal neurons: a direct patch-clamp recording study, *Nature Neuroscience* 10, 206-214.

Ngezahayo, A., Schachner, M. & Artola, A. (2000) Synaptic activity modulates the induction of bidirectional synaptic changes in adult mouse hippocampus. *J. Neurosci.* 20, 2451–2458.

Pfister, J.-P., & Gerstner, W. Triplets of spikes in a model of spike timing-dependent plasticity. *Journal of Neuroscience* 26.38 (2006): 9673-9682.

Remy, S., & Spruston, N. (2007). Dendritic spikes induce single-burst long-term potentiation. *Proceedings of the National Academy of Sciences*, 104(43), 17192–17197.

Rubin, J.E., Gerkin, R.C., Bi, G. & Chow, C.C. (2005). Calcium Time Course as a Signal for Spike-Timing Dependent Plasticity. *J Neurophysiol* 93: 2600-2613

Semon, R (1921). *The Mneme*. London: George Allen & Unwin.

Senn, W., Tsodyks, M., and Markram, H. (2001). An algorithm for modifying neurotransmitter release probability based on pre- and postsynaptic spike timing. *Neural Comput.*, 13:35-67.

Shouval, Harel Z., Mark F. Bear, and Leon N. Cooper. (2002) A unified model of NMDA receptor-dependent bidirectional synaptic plasticity. *Proceedings of the National Academy of Sciences* 99.16: 10831-10836.

Sjöström, P., Turrigiano, G., and Nelson, S. (2001). Rate, timing, and cooperativity jointly determine cortical synaptic plasticity. *Neuron* 32, 1149–1164.

Song, S., Miller, KD, and Abbott, LF (2000) Competitive Hebbian learning through spike-time-dependent synaptic plasticity. *Nature Neuroscience* 3, pp. 919–926.

Urbaniczik, R., & Senn, W. (2014) Learning by the dendritic prediction of somatic spiking. *Neuron* 81.3: 521-528.

O'Connor, D.H., Wittenberg, G.M., & Wang S.S.H. (2005) Dissection of Bidirectional Synaptic Plasticity Into Saturable Unidirectional Processes, *J Neurophysiol* 94: 1565–1573.

Wang, H.-X., Gerkin, R.C., Nauen, D.W. and G.-Q. Wang (2005) Coactivation and timing-dependent integration of synaptic potentiation and depression. *Nature Neuroscience* 8, pp. 187–193.

Xia, Z. & Storm, D. R. (2005) The role of calmodulin as a signal integrator for synaptic plasticity. *Nat.Reviews* 6, 267276.

6. Figure legends

Figure 1. Voltage-dependent plasticity model. (A) The activity $X(t)$ of the presynaptic neuron induces local dendritic voltage changes $u(t)$ in the postsynaptic neuron. Depending on the timing of the presynaptic spike, and the voltage close to the synapse, either LTP or LTD is induced. (B) The presynaptic spike $X(t)$ leaves a trace $\bar{x}(t)$ at the synapse. The voltage u is low-pass filtered with a time constant τ_+ (for the variable \bar{u}_+) or τ_- (for \bar{u}_-). The amount of LTP is proportional to \bar{x} multiplied by \bar{u}_+ , while \bar{u}_+ is above a threshold θ_+ . (C) Similarly, the amount of LTD is proportional to \bar{x} multiplied by \bar{u}_- , while \bar{u}_- is above a threshold θ_- which is lower than θ_+ and increases when LTP occurs. (D-F) Plasticity in hippocampal model cells: extracellular afferent stimulation is paired with voltage-clamp of the postsynaptic neuron at different potentials (see Ngezahayo et al., 2000). 100 brief extracellular afferent stimulations are done at 2 different frequencies: 2 (full line) and 40 Hz (dotted line). (E-F) Synaptic strength w in percentage of its initial value as a function of voltage with respect to resting potential, in mV. (G) Presynaptic trace \bar{x} (blue), voltage u (black) and its filtered version \bar{u}_+ (green full) and \bar{u}_- (orange full) for 3 different values of clamped voltage (8, 20 and 30 mV) and different stimulation frequencies. The thresholds are indicated by the dashed green (θ_+) and dashed orange (θ_-) lines. (E-G) Parameters: (E and G) $\tau_x = 5\text{ms}$, $\tau_+ = 6\text{ms}$, $\tau_- = 15\text{ms}$, $\theta_+ = 10\text{mV}$, $\theta_0 = 5\text{mV}$, $A_{LTP} = 0.0001\text{mV}^{-1}.\text{ms}^{-1}$, $A_{LTD} = 0.0001\text{mV}^{-1}.\text{ms}^{-1}$, $b_\theta = 31000\text{mV}.\text{ms}$, $\tau_\theta = 14\text{ms}$. (F) $\tau_x = 5\text{ms}$, $\tau_+ = 7\text{ms}$, $\tau_- = 15\text{ms}$, $\theta_+ = 13\text{mV}$, $\theta_0 = 7\text{mV}$, $A_{LTP} = 0.0001\text{mV}^{-1}.\text{ms}^{-1}$, $A_{LTD} = 0.0001\text{mV}^{-1}.\text{ms}^{-1}$, $b_\theta = 45000\text{mV}.\text{ms}$, $\tau_\theta = 5\text{ms}$.

Figure 2. Subthreshold plasticity at CA3 synapses in the hippocampus. (A) Experimental setup. Stimulations of CA3 recurrent inputs (blue electrode) are followed (10ms) or preceded (-40ms) by stimulations of mossy fiber (MF, brown electrode). (B) Voltage traces following subthreshold stimulations. Left+middle: stimulations with a 10ms interval: two types of voltage responses were recorded in the dendrite (black electrode in A): linear (left) and supralinear (middle) ones. The supralinear responses correspond to the occurrence of dendritic spikes. Right: stimulations with a -40 ms interval. Time of presynaptic stimulation is set to 0. Top panel: presynaptic trace $\bar{x}(t)$. Middle panel: filtered voltage (\bar{u}_+ and \bar{u}_- in orange and green full lines, respectively). The thresholds are indicated by the dashed green (θ_+) and orange (θ_-) lines. Lower panel: the synaptic weight w . (C) Plasticity outcome for 3 cells using 5 different protocols: CA3 stimulation only, no pairing; subthreshold protocol with different time intervals (0 ms, 10 ms, -40 ms) and, for the 10 ms time interval, in the presence of the NMDA blocker AP5 (10ms, block). Filled circles represent data from individual cells. Red crosses represent simulations using the parameters obtained with the best fit. Note that the plasticity model had the same parameters for all cells. Differences in plasticity arise due to differences in experimental voltage traces. For -40ms, representative voltage time course were recorded from two of the three cells, but plasticity was not measured. We used the averaged value obtained during this protocol in a different set of cells (open circles). Data shared by F. Brandalise. (D) Least Squared Error (LSE) of the best fit subtracted from the LSE obtained after increasing (upper panel) or decreasing (lower panel) each parameter by 10%, one parameter at a time (ΔLSE).

Figure 3. Variation of the least square error (LSE) as a function of parameter change. (A) LSE (vertical axis) when all the parameters were increased or decreased (horizontal axis) by a fixed percentage. (B) Only the parameter τ_x is changed (horizontal axis) by a fixed percentage. (C) Filled contour plot of the LSE while 2 parameters are increased or decreased by a given percentage: τ_+ & θ_+ (C1), τ_- & θ_0 (C2), A_{LTP} & A_{LTD} (C3) b_θ & τ_θ (C4). (D) Plasticity

value for 3 cells in 5 different conditions (see Figure 2). Circles represent data from individual cells. Red crosses represent simulations using the parameters obtained with the best fit. Grey symbols in D represent simulations using the parameters obtained with the best fit except a few which were changed by a certain percentage (lower panel) or when all parameters were changed by a fixed percentage (upper panel, compare symbols in A, B, C1-C4): boxed and unboxed star in A (-2 and +4%, respectively), hexagon in B (-5%), upwards-pointing triangle in C1 (+9% and -3%), rectangle in C2 (-9% and +5%), cross in C3 (+15% and +15%), and downwards-pointing triangle in C4 (-70% and -30%).

Figure 4. Spike-timing dependent plasticity at CA3 synapses. (A) STDP protocol (Brandalise et al. 2016): stimulations of CA3 recurrent inputs were paired 50 times with brief somatic current injections (2 ms; 4 nA) to evoke action potentials (APs). (B-C-D) Glutamate trace $\bar{x}(t)$ (blue), and representative traces of the voltage u (black) as a function of time. The model variables \bar{u}_+ (green full line), \bar{u}_- (orange full line), θ_+ (green dashed line) and θ_- (green dashed line) are plotted for the full voltage trace. (B) When 3 APs were evoked at a frequency of 200 Hz, dendritic spikes (full line) occurred in 60% of the trials. In the remaining 40%, a linear response was generated (dashed line). (C) Dendritic spikes were completely abolished when a hyperpolarizing pulse was applied. (D) Responses were always linear, if the frequency of AP was lowered to 50 Hz (full line) or only one AP was paired with stimulation of CA3 recurrent inputs (dashed line). (E) Plasticity during the STDP protocol: black error bars represent data from Brandalise et al. (2016) and red crosses simulations. All data points in E are fitted with a single set of parameters (see main text and Table 2).

Figure 5. Distance-dependent STDP at synapses between layer 2/3 and layer 5 pyramidal neurons in somatosensory cortex. (A) Experimental voltage trace at proximal (bottom panels) and distal (top panels) synapses. Postsynaptic bursts (3 action potentials, APs at 200 Hz) are paired with presynaptic action potentials (± 10 ms time interval, pairing frequency of 1 Hz). (B) Plasticity along the dendrite for the protocol described in A: 1 pre-3 APs (left) or 3 APs-1 pre (right). EPSP rise time is a proxy of the distance between the plastic synapse and the soma. See text for more details. (C-D) Voltage (C) and plasticity (D) are measured at distal synapses, in the presence or absence of NiCl_2 (blocks T- and/or R-type voltage-gated calcium channels). Crosses and dots or crosses with error bars represent plasticity from Letzkus et al. (2006) and red lines simulations. Voltage traces are redrawn from Letzkus et al. (2006).

Figure 6. Components of the model for distal neocortical synapses. (A-C) Glutamate trace \bar{x} (top), voltage u and its filtered version \bar{u}_+ and \bar{u}_- (middle), w , dw_{LTP} and dw_{LTD} (bottom) as a function of time ($w(t) = w(t-1) + dw_{\text{LTP}} + dw_{\text{LTD}}$). The blue dashed line corresponds to the dw_{LTD} when b_θ is set to 0 (no veto, bottom). The voltage time course u is redrawn from Letzkus et al., 2006 (see also Figure 5). (A) During +10 ms pairings, the value of the presynaptic trace \bar{x} has already decreased half when \bar{u}_+ reaches θ_+ . The amount of LTP is not high enough for the veto to have a significant impact on LTD induction. (B) In contrast, for -10 ms pairings, \bar{x} switches from 0 to its maximal value 1 at around the time when \bar{u}_+ reaches its maximal value far above θ_+ and \bar{u}_- is slightly above θ_- . Therefore, the amount of LTP induced is high and significantly reduces LTD via an increase of the LTD threshold θ_- . (C) However, in the presence of NiCl_2 , the difference between \bar{u}_+ and θ_+ is significantly reduced compared to the control case in B, leading to a similar behavior of the plasticity model than described for the +10ms pairings.

Figure 7. Pairing and timing-dependence of plasticity at neocortical synapses. (A) Two synaptically connected L5 neurons were stimulated with different time intervals (-10, 0, 10 and 25 ms) at different pairing repetition frequencies: 0.1 Hz, 10 Hz, 20 Hz and 40 Hz. (B) Simulated dendritic (black), somatic (purple) and experimentally recorded somatic (blue) voltage time course for +10 ms time interval. The experimental voltage trace is redrawn from Sjöström et al. (2001); inset: simulated EPSP time course. (C) Plasticity as a function of spike

timing. Each panel represents one pairing repetition frequency. Black errorbars represent data from Sjöström et al. (2001) and red squares represent our plasticity model. (D, E) Presynaptic trace \bar{x} (blue), voltage u (black) and its filtered version \bar{u}_+ (green) and \bar{u}_- (orange) for +10 ms time interval: 0.1 Hz (D) or 20 Hz (E) repetition frequency.

Table 1. Protocol 3 and 4 (+10ms) for cells 1-3. Rise time of EPSP, increase of EPSP amplitude during supralinear events, percentage of supralinear events and amount of potentiation of the 3 recorded cells. The occurrence of supralinear events was completely blocked by AP5 infusion ("block", cell 1) or holding the cell at -90 mV ("block", cell 3). The % increase amplitude is defined as the difference between the amplitude a_s of the supralinear events and the amplitude a_l of the linear events, divided by the amplitude of the linear events: $\% = 100(a_s - a_l) / a_l$. Note that a value of 100 indicates a maximum voltage twice as high as predicted by linear summation.

Table 2. Parameters giving the smallest error (see Methods). The error is defined as the squared difference between experimental and theoretical value.

Table 3. Median error after training on 11 plasticity traces and testing on the 12th excluded one. Training is the averaged error divided by 11. We obtain 12 sets of best parameters after the cross-validation: we indicate here the coefficient of variation for each parameter ($sd/mean*100$).

Table 4. Lower and upper bound used during the fmincon search

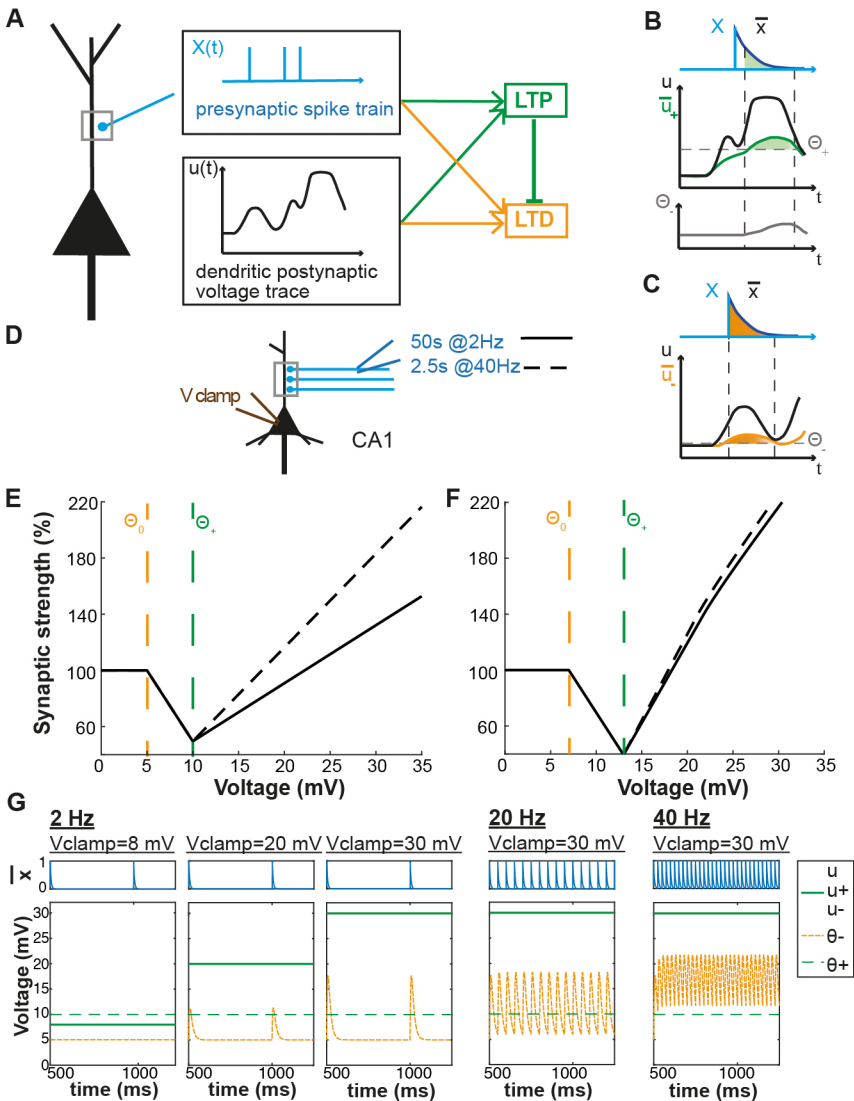


Figure 1

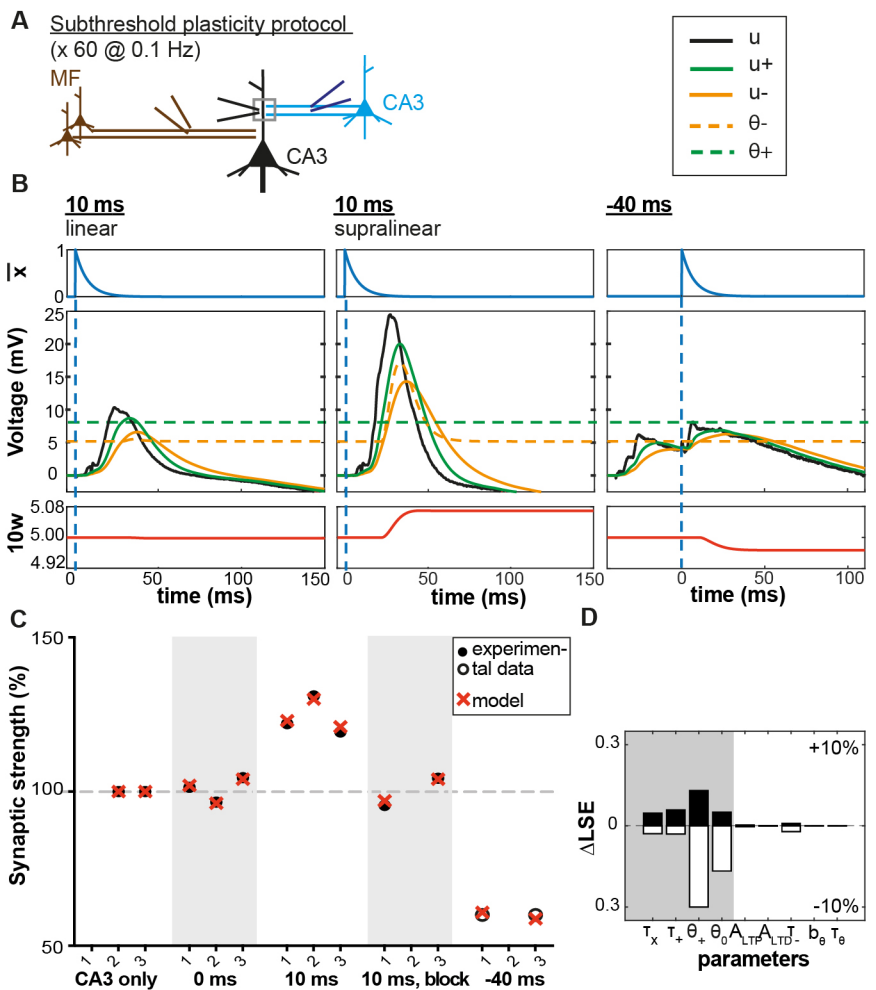


Figure 2

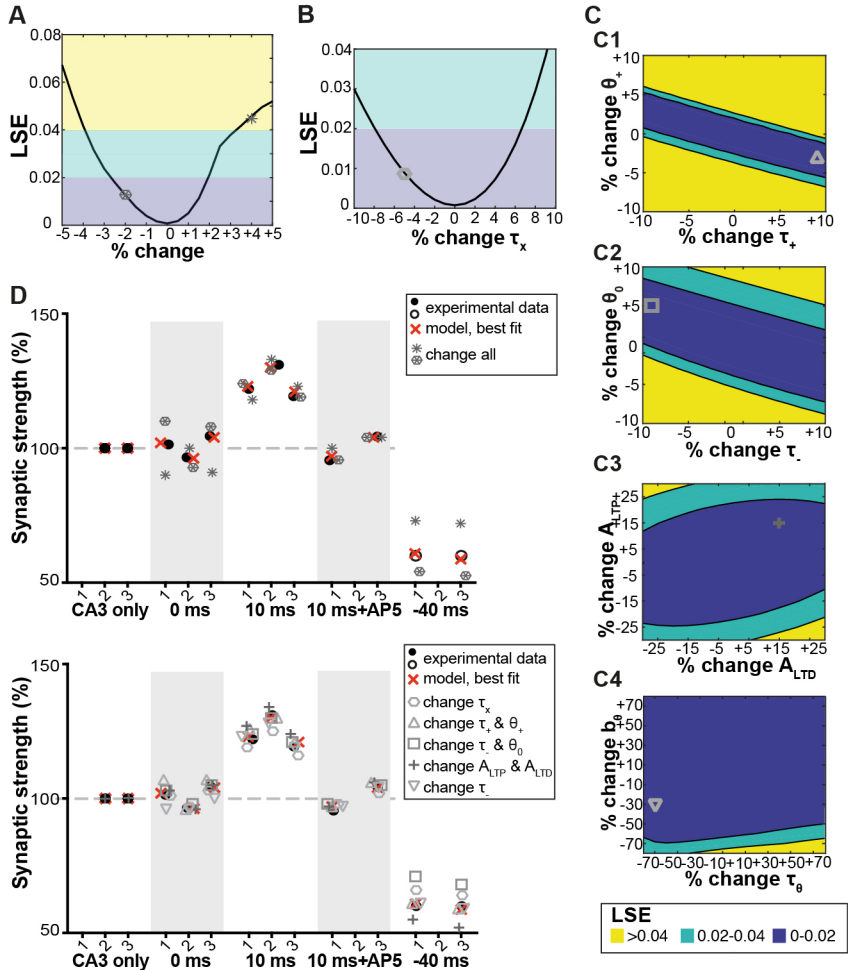


Figure 3

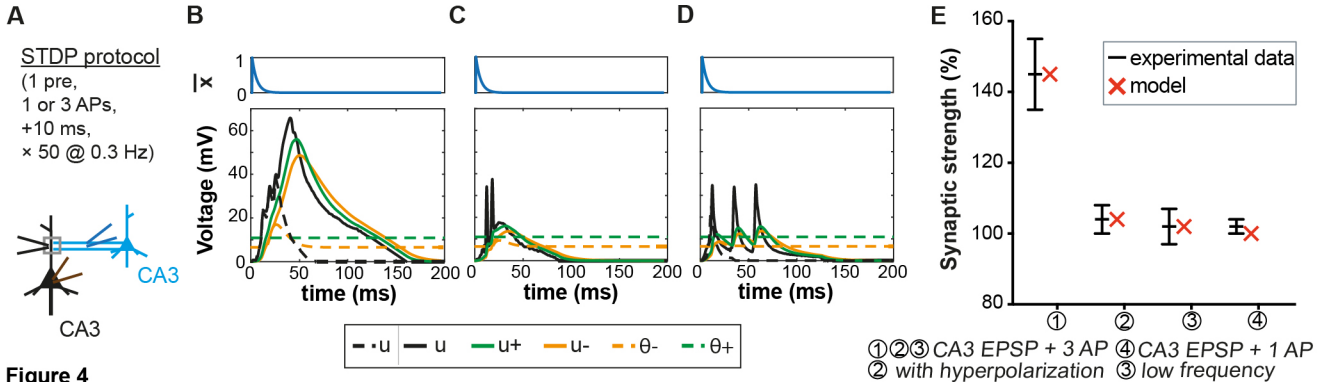


Figure 4

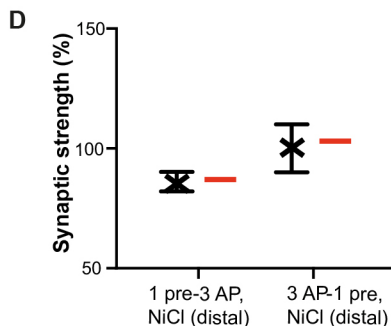
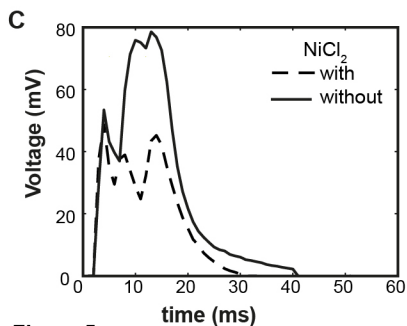
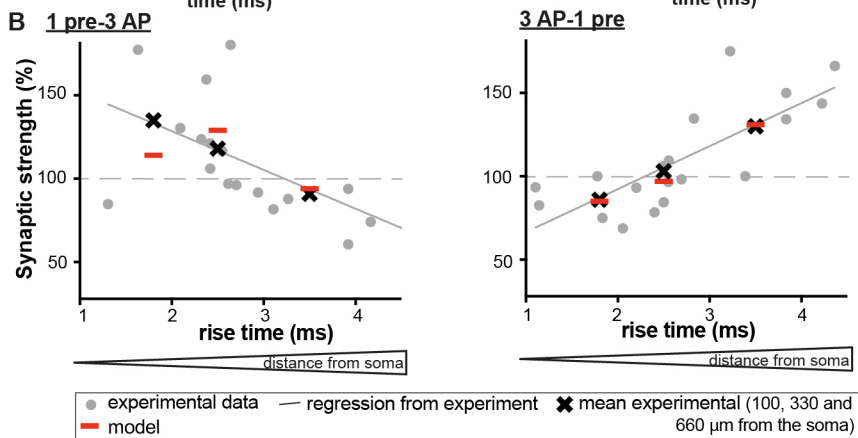
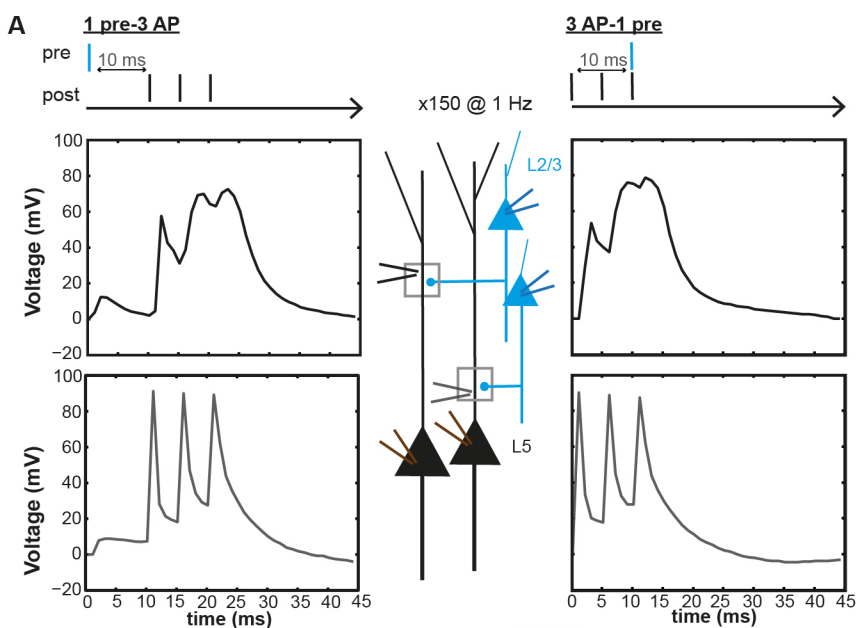


Figure 5

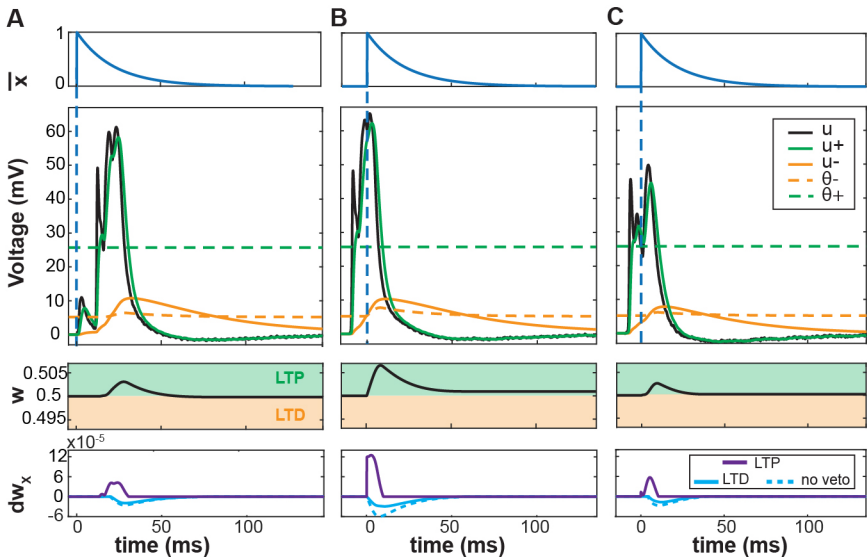
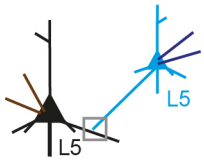
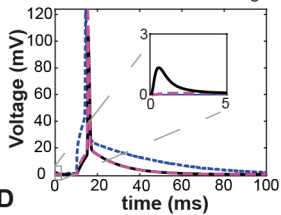


Figure 6

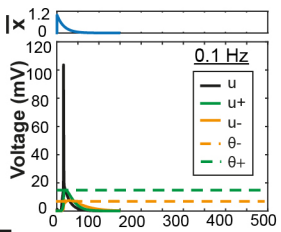
A STDP protocol: 1 pre-1AP
 x 60 @ 0.1 Hz
 x5 @ 10, 20 or 40 Hz, 15 repeats)



B
 --- experimental somatic voltage
 - - - simulated somatic voltage
 — simulated dendritic voltage



D



E

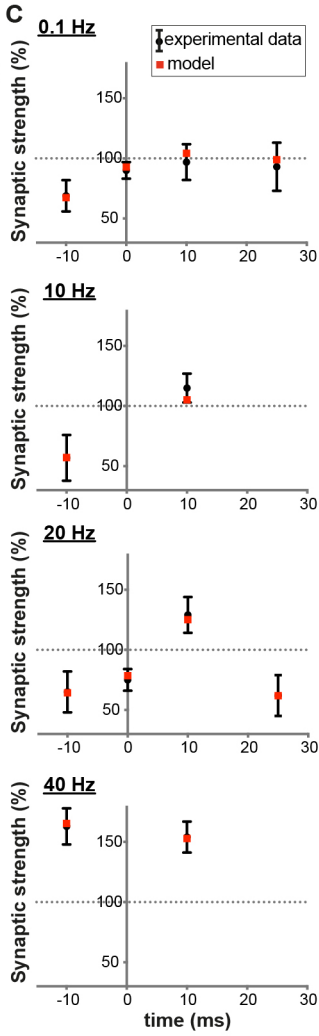
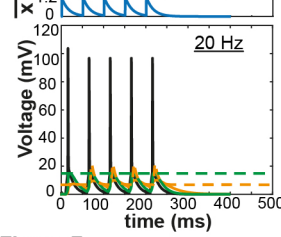


Figure 7